

Contents lists available at ScienceDirect

# Journal of the Mechanical Behavior of Biomedical Materials

journal homepage: http://www.elsevier.com/locate/jmbbm





# Glycosaminoglycan depletion increases energy dissipation in articular cartilage under high-frequency loading

Guebum Han<sup>a</sup>, Utku Boz<sup>a</sup>, Melih Eriten<sup>a</sup>, Corinne R. Henak<sup>a,b,c,\*</sup>

- <sup>a</sup> Department of Mechanical Engineering, University of Wisconsin-Madison, 1513 University Ave., Madison, WI, 53706, USA
- b Department of Biomedical Engineering, University of Wisconsin-Madison, 1550 University Ave., Madison, WI, 53706, USA
- <sup>c</sup> Department of Orthopedics and Rehabilitation, University of Wisconsin-Madison, 1111 Highland Ave., Madison, WI, 53705, USA

## ARTICLE INFO

#### Keywords: Energy dissipation Glycosaminoglycan Osteoarthritis High-frequency loading Ouasi-static loading

#### ABSTRACT

High-frequency material behavior of cartilage at macroscopic lengths is not widely understood, despite a wide range of frequencies and contact lengths experienced *in vivo*. For example, cartilage at different stages of matrix integrity can experience high-frequency loading during traumatic impact, making high-frequency behavior relevant in the context of structural failure. Therefore, this study examined macroscopic dissipative and mechanical responses of intact and glycosaminoglycan (GAG)-depleted cartilage under previously unexplored high-frequency loading. These dynamic responses were complemented with the evaluation of quasi-static responses. A custom dynamic mechanical analyzer was used to obtain dynamic behavior, and stress relaxation testing was performed to obtain quasi-static behavior. Under high-frequency loading, cartilage energy dissipation increased with GAG depletion and decreased with strain; dynamic modulus exhibited opposite trends. Similarly, under quasi-static loading, equilibrium modulus and relaxation time of cartilage decreased with GAG depletion. The increased energy dissipation after GAG depletion under high-frequency loading was likely due to increased viscoelastic dissipation. These findings broaden our understanding of fundamental properties of cartilage as a function of solid matrix integrity in an unprecedented loading regime. They also provide a foundation for analyzing energy dissipation associated with cartilage failure induced by traumatic impact.

## 1. Introduction

Articular cartilage is a load-bearing and dissipative material that cushions the ends of bones in diarthrodial joints and protects against load-induced damage. The cartilage solid matrix is made of proteoglycans (PGs) with sulfated glycosaminoglycan (GAG) side chains (4–7% of wet weight (Mow et al., 1992)) embedded in a dense collagen fibril matrix (15–22% of wet weight (Mow et al., 1992)). While collagen fibrils under tension maintain cartilage integrity (Andriotis et al., 2018; Eisenberg and Grodzinsky, 1985; Kempson et al., 1968; Soulhat et al., 1999), negatively charged GAGs provide positive swelling force and compressive resistance through osmotic pressure and repulsive interactions between charge groups (Han et al., 2011; Mow et al., 1992). The largest component of cartilage is fluid (about 60–85% of wet weight), which swells the solid matrix and pore space (Maroudas et al., 1991; Mow et al., 1992; Torzilli, 1985).

Dissipative and mechanical responses of cartilage arise due to poroelastic (PE) and intrinsic viscoelastic (VE) relaxations (Akizuki

et al., 1986; Boettcher et al., 2016; Han et al., 2018; Matthews et al., 1977; Nia et al., 2011). PE relaxation is caused by drag due to stress-induced pore fluid diffusion, resulting in energy dissipation via fluid-solid frictional interaction (Mow et al., 1980). PE relaxation time depends on a characteristic diffusion length and diffusivity (DiDomenico et al., 2018; Han et al., 2018; Lai and Hu, 2017; Nia et al., 2011, 2013). Intrinsic VE relaxation is induced by interactions and rearrangement of solid matrix macromolecules (Huang et al., 2003; Lakes, 2009; Mak, 1986). Therefore, VE relaxation time is length- and diffusion-independent at the continuum level (Han et al., 2018; Lai and Hu, 2017; Mak, 1986). PE and VE relaxation mechanisms both play important roles in dissipative capacity and protection against failure of cartilage (Edelsten et al., 2010; Fulcher et al., 2009; Han et al., 2019; Lawless et al., 2017; Nia et al., 2011, 2013, 2015).

Although dissipative and mechanical responses of cartilage at microscale lengths have been explored up to high frequencies as a function of solid matrix integrity, they are only partially understood at macroscopic lengths. At microscale lengths, GAG-depleted cartilage has

<sup>\*</sup> Corresponding author. Department of Mechanical Engineering, University of Wisconsin-Madison, 1513 University Ave., Madison, WI, 53706, USA. E-mail addresses: ghan28@wisc.edu (G. Han), utkuboz87@gmail.com (U. Boz), eriten@wisc.edu (M. Eriten), chenak@wisc.edu (C.R. Henak).

higher permeability due to increased pore size, resulting in lower dynamic modulus and an increase in the frequency of peak PE dissipation in the 1-10 kHz range (Nia et al., 2013). In the 5-100 Hz range, VE provides a baseline for dissipation, while PE dissipation increases overall dissipation at relatively small length scales (Han et al., 2018). Under quasi-static loading at microscale lengths, elastic moduli of GAG-depleted cartilage are much lower than those of intact cartilage across the full-thickness sample, but permeability shows an opposite trend (Wahlquist et al., 2017). These previous studies provide dissipative and mechanical responses of cartilage at microscale lengths over a broad frequency range corresponding to walking (1-8 Hz), running (4–100 Hz), jumping (2–100 Hz), and traumatic impact (≥200 Hz) (Nia et al., 2013). However, cartilage responses at macroscale lengths ( $\geq 2$ mm) have only been partially explored in a relatively low-frequency range. For example, storage and loss moduli of intact cartilage gradually reach constant values at around 15 Hz and maintain them up to around 90 Hz, and higher applied stresses decrease phase shift (Fulcher et al., 2009; Lawless et al., 2017). Decreased solid matrix integrity decreases modulus and increases phase shift under shear at 0.1 Hz and compressive loading from 0.1 Hz to 40 Hz (Griffin et al., 2014; Park et al., 2008). To date, macroscopic dissipative and mechanical responses of cartilage as a function of solid matrix integrity and strain have not been investigated under high-frequency normal loading ( $\geq$  40–90 Hz). This gap is important to fill because in vivo contact occurs at macroscale lengths (Chan et al., 2016; Fukubayashi and Kurosawa, 1980) and includes high-frequency loading during traumatic impact (Nia et al., 2013). Previous studies show that cartilage failure can be easily induced under relatively fast loading rates (Bartell et al., 2018; G. Han et al., 2019; Henak et al., 2017; Kaplan et al., 2017; Sadeghi et al., 2015). The measurement of fundamental cartilage behavior under high-frequency loading can lay the foundation for understanding cartilage failure induced under traumatic loading scenarios.

The aim of this study is to fill this gap by examining the effects of solid matrix integrity and strain on dissipative and mechanical responses of cartilage up to 300 Hz in order to cover previously unexplored trauma scenarios under macroscopic contact lengths.

#### 2. Methods

Cartilage dynamic and quasi-static behavior was evaluated as a

function of solid matrix integrity (Fig. 1). Dynamic responses were measured by using a dynamic mechanical analyzer (DMA). Quasi-static responses were measured by performing stress relaxation tests.

# 2.1. Sample preparation: intact cartilage

Patellae from eight porcine joints were harvested from a local abattoir (8 animals, 5–6 months old, sex unknown and assumed random). A total of 16 cylindrical cores with a diameter of 4 mm were obtained using a biopsy punch and a scalpel (two cylindrical cores per animal). A microtome was used to remove subchondral bone and achieve a deep surface parallel to the articular surface. Eight of the total 16 cores were used to measure dynamic responses of intact and GAG-depleted cartilage, and the others were used to measure the quasistatic responses (Fig. 1). Cartilage samples were kept hydrated during the preparation process in Dulbecco's phosphate-buffered saline (DPBS) with a protease inhibitor (PI) (Pierce Mini Tablets, EDTA-free, Thermo Fisher, Waltham, MA).

# 2.2. Quasi-static testing

Quasi-static responses of intact and GAG-depleted cartilage were examined by measuring stress relaxation responses under unconfined compression at four different strain levels (Fig. 1a-c). Tests were conducted on a 3230-AT Series III test instrument (TA Instruments, New Castle, DE) with a 6 mm diameter flat indenter. Intact cartilage was attached to a stage, compressed up to 5% strain with a  $0.1 \, \mathrm{s}^{-1}$  strain rate, and relaxed for 11 min. The relaxation time was selected to make sure that cartilage reached equilibrium after 10-min relaxation at which time dynamic testing was performed. Additional steps of 5% strain and holding period were repeatedly applied up to 20% strain. After testing intact cartilage, mild-GAG-depletion was induced via a 30 min incubation period in 0.25% trypsin at 37 °C, and the test protocol used for intact cartilage was conducted. Severe-GAG-depletion was then induced via an additional 6.5-h incubation in 0.25% trypsin at 37 °C, and the testing was repeated. Trypsin digests the non-fibrillar matrix which is mostly made of PGs with core proteins and GAG chains (Griffin et al., 2014; Nguyen et al., 1989), but it does not significantly affect the micro/macroscale structural features and tensile strength of the collagen fibrillar matrix (Bonassar et al., 1995; Lewis and Johnson, 2001;

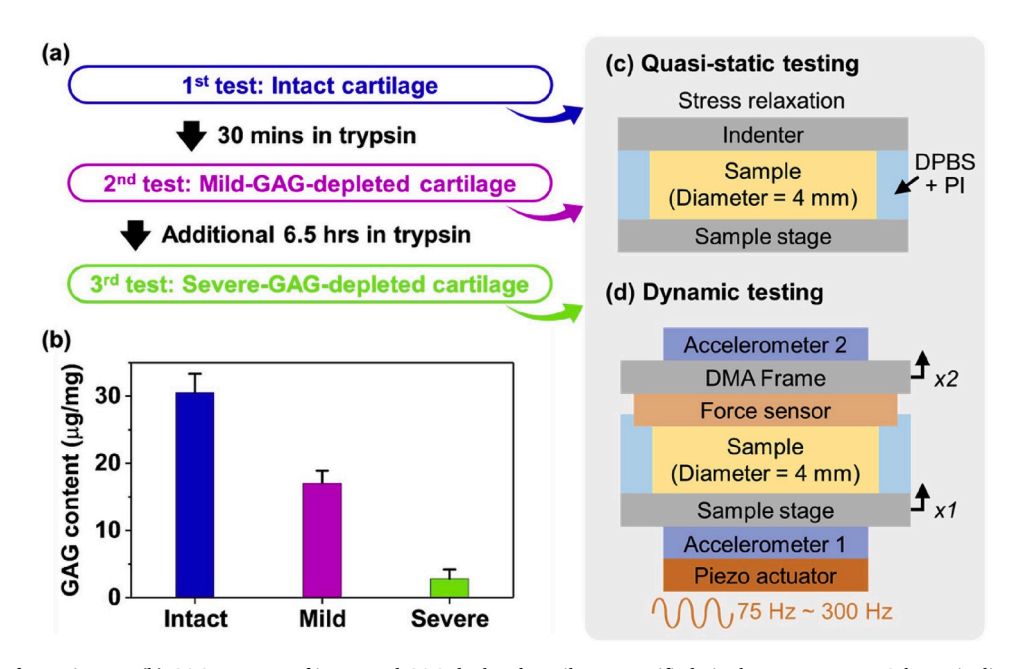


**Fig. 1.** (a) Overview of experiments. (b) GAG contents of intact and GAG-depleted cartilage quantified via the DMMB assay. Schematic diagrams of (c) quasi-static (stress relaxation) and (d) dynamic testing setups. (c) and (d) are not drawn to scale. The error bars in (b) show the standard deviations (n = 4).

Schmidt et al., 1990). GAG contents after trypsin treatments were quantified in pilot samples (n = 4) subjected to a dimethylmethylene blue (DMMB) assay (intact:  $30.55 \pm 2.77 \, \mu g/mg$  wet weight, PG depletion for 30 min:  $17.07 \pm 1.83 \, \mu g/mg$  wet weight, and PG depletion for additional  $6.5 \, h$ :  $2.84 \pm 1.35 \, \mu g/mg$  wet weight) (Fig. 1b). After each trypsin treatment, cartilage samples were immersed in DPBS with a PI for around 1 h to reach equilibrium. Cartilage thickness was then measured using calipers, and the average thickness (n = 8) was  $1.61 \pm 0.21 \, \text{mm}$ . Consistent with a previous study (Huang and Zheng, 2009), the effect of GAG depletion on cartilage thickness was negligible.

Stress relaxation responses were used to quantify peak stresses, equilibrium moduli, and relaxation times of intact and GAG-depleted cartilage. First Piola-Kirchhoff peak stress for each strain level was calculated by dividing the peak load (unrelaxed state) with reference configuration area,  $A = \pi r^2 = 12.57 \text{ mm}^2$ . Equilibrium stress was calculated by dividing equilibrium load (relaxed state) by A. Equilibrium load for each strain was defined as the load response after 10 min of relaxation (Fig. 2a) because there was virtually no further relaxation; load relaxation between 10 min and 11 min was less than 0.08% of total relaxation defined as from peak load to equilibrium load for each strain. A linear function was fitted to average equilibrium stresses as a function of strain, and its slope represented the equilibrium modulus of cartilage. Relaxation time was defined as the time required to relax 90% of the total relaxation.

# 2.3. Dynamic testing under high-frequency loading

Macroscopic dynamic responses of intact and GAG-depleted cartilage under high-frequency loading were investigated by measuring the phase shift and dynamic modulus using the DMA (Fig. 1a,b, and d). Intact cartilage was compressed to 5% strain and relaxed for 10 min to reach equilibrium (relaxed state) (Fig. 2a). Then, a frequency sweep from 75 Hz to 300 Hz with a small oscillation (about 650 nm) was applied to a

sample stage using a piezo actuator (PI P-250.20, PI, Auburn, MA). Dynamic testing was repeated at 10, 15, and 20% strain, with strain levels matched to the quasi-static testing. Acceleration of the sample stage and DMA frame induced by the piezo actuator was measured with two accelerometers (PCB333B30, PI, Auburn, MA) (Fig. 1d). Displacements for the sample stage, x1, and DMA frame, x2, were obtained from the double integration of their measured acceleration. The force response during the frequency sweep was measured by a dynamic force sensor (PCB208C01, PI, Auburn, MA). The sampling frequency for measuring the acceleration and force was 5 kHz. Using these measured responses, the complex dynamic stiffness,  $K(\omega)$ , was obtained through the frequency domain analysis as follows:

$$K(\omega) = \frac{F(\omega)}{X1(\omega) - X2(\omega)} \tag{1}$$

where  $F(\omega)$  is the force response and  $X1(\omega)$  and  $X2(\omega)$  are the displacements of the sample stage and DMA frame, respectively, in the frequency domain. Then, the complex dynamic modulus,  $E(\omega)$ , was calculated as follows:

$$E(\omega) = \frac{K(\omega)l_c}{A} \tag{2}$$

where  $l_c$  is the thickness of cartilage at each stain level and A is the reference configuration contact area between the force sensor and cartilage. As the diameter of the force sensor was larger than that of cartilage, A was equal to the area of articular surface. The magnitude,  $|E(\omega)|$ , and phase,  $\angle E(\omega)$  provided the dynamic modulus and phase shift of intact cartilage, respectively. Following intact cartilage, mild-GAG-depleted and severe-GAG-depleted cartilage were tested using the same test protocol in consecutive order. GAG-depleted samples were prepared in the same way as those used for the quasi-static testing. The average cartilage thickness (n = 8) used for dynamic testing was

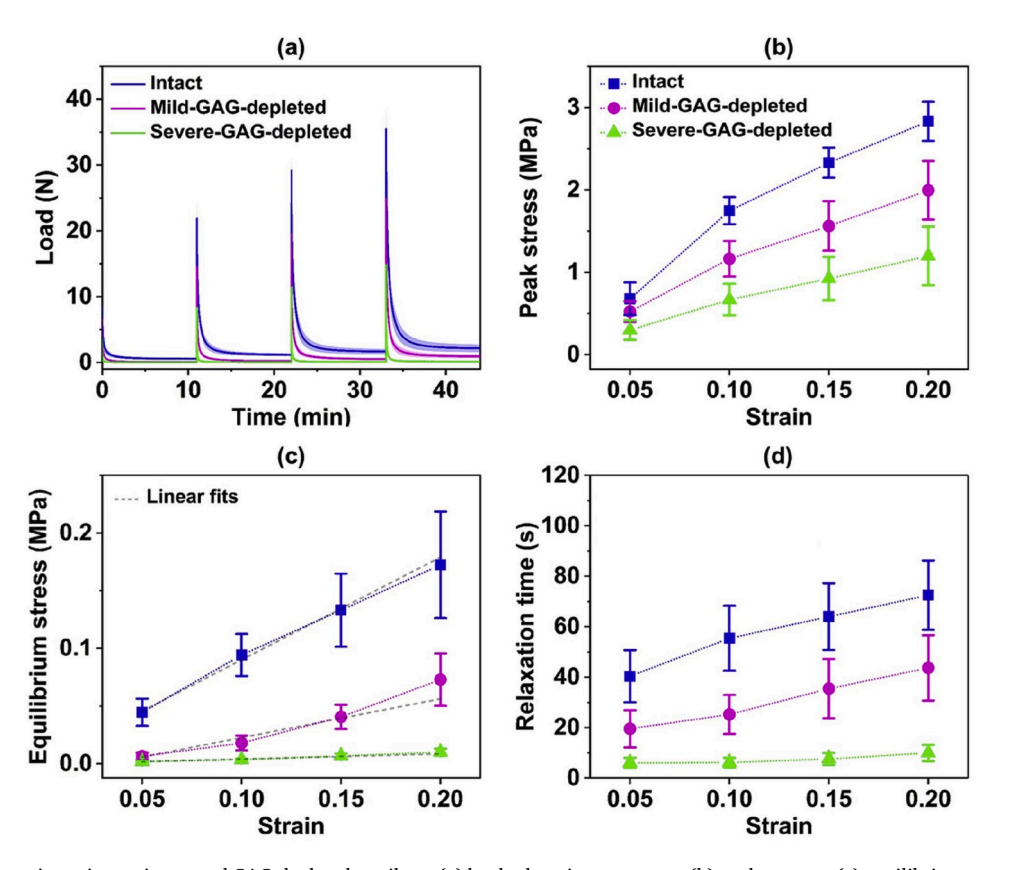


Fig. 2. Results of quasi-static testing on intact and GAG-depleted cartilage: (a) load relaxation responses, (b) peak stresses, (c) equilibrium stresses, and (d) relaxation times. The shaded error bands in (a) and error bars in (b), (c), and (d) show the standard deviations (n = 8).

#### 1.72±0.22 mm.

#### 2.4. Statistical analysis

Data were not normally distributed and were therefore subjected to nonparametric analysis. A two-way aligned rank transformation analysis of variance (ART ANOVA) was used to assess the effects of both GAG depletion and strain on peak stress, equilibrium stress, relaxation time, phase shift, and dynamic modulus, as well as the effects of frequency on phase shift and dynamic modulus. Pairwise analysis compared different strain levels and GAG depletion levels using post-hoc Tukey-corrected pairwise tests. Statistical analyses were performed in R 3.6.0, and a significance level of 0.05 was used.

#### 3. Results

Quasi-static peak stresses, equilibrium stresses, and relaxation times of cartilage increased with strain and decreased with GAG depletion (Fig. 2a). Peak stresses of intact cartilage depended on GAG depletion (p < 0.0001). Intact cartilage had larger peak stresses than both mild-GAGdepleted and severe-GAG-depleted cartilage (p < 0.0001). Peak stress values in intact cartilage at 5% and 20% strain 2.28 times and 2.37 times larger than those of severe-GAG-depleted cartilage, respectively (Fig. 2b). Equilibrium stresses of cartilage decreased with GAG depletion (p < 0.0001) and increased with strain (p < 0.0001), with significance between all pairs (p < 0.003) (Fig. 2c). Intact cartilage at 5% and 20% strain exhibited 25.05 times and 17.33 times larger equilibrium stresses than severe-GAG-depleted cartilage, respectively. Equilibrium stresses of intact and severe-GAG-depleted cartilage at 20% strain were 3.87 times and 5.58 times higher than those at 5% strain, respectively. From the slopes of the linear fits (Fig. 2c), equilibrium moduli of intact, mild-GAG-depleted, and severe-GAG-depleted cartilage were 0.89 MPa (R<sup>2</sup> > 0.99), 0.34 MPa ( $R^2 = 0.94$ ), and 0.05 MPa ( $R^2 = 0.97$ ), respectively. Relaxation times of cartilage reduced with GAG-depletion (p < 0.0001) and increased with strain (p < 0.0001) (Fig. 2d). All pairwise comparisons by GAG level were significant (p < 0.0001). Severe-GAG-depleted cartilage at 5% and 20% strain relaxed 6.74 times and 7.28 times faster than intact cartilage. Relaxation times of intact and severe-GAGdepleted cartilage from 5% strain to 20% strain increased 1.8 times and 1.66 times, respectively (p < 0.0001 between strain levels). Increasing relaxation times with strain and decreasing relaxation times with GAG depletion were consistent with previous studies (Han et al., 2011; June et al., 2009; Kiviranta et al., 2006; Korhonen et al., 2002); some differences in relaxation times could be due to loading conditions, the definition of relaxation times, age, and species of samples.

High-frequency phase shifts and dynamic moduli of cartilage depended on GAG-depletion and strain (Fig. 3). Phase shifts of cartilage increased with GAG depletion (p < 0.0001) and decreased with strain (p < 0.0001). All pairwise comparisons by GAG level were significant (p < 0.0001). For example, at 200 Hz under 5% strain, phase shifts increased from about 7.37° to about 12.91° after inducing severe-GAGdepletion. Phase shifts at 200 Hz decreased about  $1.5^{\circ}$  from 5% strain to 20% strain for intact cartilage, and this decreasing trend was also observed in mild- and severe-GAG-depleted cartilage (p < 0.0001 between strain levels). Phase shifts of intact and GAG-depleted cartilage were statistically rate-dependent in the high-frequency range of interest (p < 0.0001), but the numerical values only increased about one degree from 75 Hz to 300 Hz. In contrast to trends in phase shifts, dynamic moduli of cartilage decreased with GAG depletion (p < 0.0001) and increased with strain (p < 0.0001). For instance, dynamic moduli of intact cartilage at 5% strain at 200 Hz (32.79 MPa) were 2.6 times larger than those of severe GAG-depleted cartilage at 5% strain (12.49 MPa) (p < 0.0001 between GAG depletion levels). From 5% strain to 20% strain, dynamic moduli of intact and severe-GAG-depleted cartilage increased about 1.35 times and about 1.48 times, respectively (p < 0.0001 between strain levels).

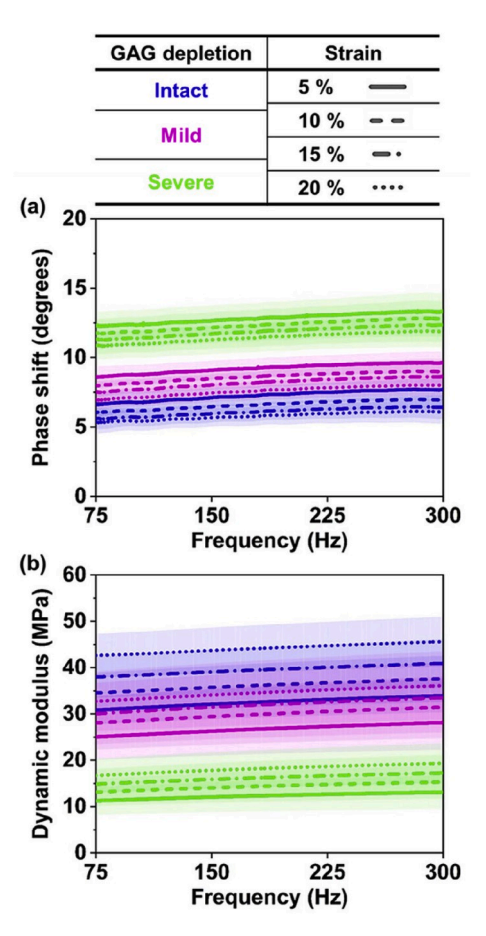


Fig. 3. (a) Phase shifts and (b) dynamic moduli of intact and GAG-depleted cartilage under high-frequency loading (75–300 Hz). The shaded error bands show the standard deviations (n=8).

# 4. Discussion

Macroscopic energy dissipation of intact cartilage originates predominantly from intrinsic VE dissipation under high-frequency loading. Cartilage undergoes nearly isochoric deformation with the restricted fluid flow when a PE Peclet number (defined as the ratio of the PE relaxation time constant to the inverse of the applied strain rate (Quinn et al., 2001)) is larger than 1. PE relaxation time is proportional to the square of a characteristic length but inversely proportional to diffusivity (Hu et al., 2010; Nia et al., 2011). Therefore, PE Peclet number for intact cartilage in this study can be estimated from published diffusivity, 3.89  $\times$  10<sup>-11</sup> m<sup>2</sup>/s (Han et al., 2018), the sample dimensions (2 mm radius) and the strain rate ( $\dot{\varepsilon} = 0.11 \text{ s}^{-1}$  at 75 Hz and 0.45 s<sup>-1</sup> at 300 Hz) as much larger than 1. This suggests that VE dissipation dominates the measured relaxation. In addition, our previous study with dynamic testing at multiple contact radii showed that the energy dissipation of intact cartilage at a contact radius of about 40  $\mu m$  was dominated by intrinsic VE dissipation under oscillatory loading (5-100 Hz with a small amplitude of around 1.25 nm) (Han et al., 2018). As the contact radius, frequency, and amplitude of the current study were larger than those of the previous study, intact cartilage likely behaved as a nearly incompressible solid and dominantly dissipated energy through intrinsic VE dissipation. Further, the measured phase shift (about 7° at 5% strain) was consistent with that of intrinsic VE dissipation reported in the previous work (about 8° at 0.8% representative strain) in the overlapped frequency range (75-100 Hz) (Han et al., 2018); samples used for both studies had the same age and species and were also harvested from the same local abattoir. Strain- and frequency-dependent phase shift of intact cartilage were consistent with macroscopic VE properties

reported in previous studies (1–92 Hz) (Fulcher et al., 2009; Lawless et al., 2017); some minor discrepancies in phase shift were likely due to species, age, and test conditions.

GAG depletion enhanced the energy dissipation of cartilage under high-frequency loading. GAG-depleted cartilage exhibited a higher phase shift than intact cartilage, showing that the loss of GAG content increases energy dissipation (Fig. 3a). GAG depletion was likely to increase intrinsic VE dissipation. A previous study under shear loading (0.1 Hz) where there are virtually no poroelastic effects showed that GAG depletion increased cartilage dissipation (Griffin et al., 2014). In the current study, poroelastic effects were also minor even after GAG deletion due to the high-frequency compressive loading at a macroscopic characteristic diffusion length; the Peclet number for GAG-depleted cartilage was also much larger than 1, which was estimated with the current loading condition, measured representative modulus (0.05 MPa), and previously reported permeability for GAG-depleted cartilage (1.3  $\times$  10<sup>-13</sup> m<sup>4</sup>/N·s (Nia et al., 2013)). Therefore, the current study combined with the previous study implies that VE dissipation, stemming from macromolecular rearrangement and interactions within the solid matrix (Huang et al., 2003; Lakes, 2009; Mak, 1986), increases high-frequency macroscopic cartilage dissipation after GAG depletion. In addition, as GAG depletion increases diffusivity (Nia et al., 2013; Wahlquist et al., 2017) without affecting the collagen fibril matrix (Griffin et al., 2014; Nguyen et al., 1989), there could be a minor contribution of altered PE dissipation to the difference in phase shifts of intact and GAG-depleted cartilage. While PE dissipation in intact cartilage was likely to come from frictional interactions between GAGs and fluid (Nia et al., 2015), PE dissipation of GAG-depleted cartilage was likely to originate from frictional interactions between collagen fibrils and fluid. Moreover, since GAG depletion significantly decreased dynamic (around 2.5 times) and equilibrium (around 18 times) moduli and increased diffusivity, interfacial dissipation between the indenter and tissue, squeeze film damping effects, and flow near the edge of cartilage might have minor contributions to the increased cartilage dissipation. These results imply that osteoarthritis, which includes GAG loss, could increase macroscopic energy dissipation of cartilage under high-frequency loading.

The degeneration of the solid matrix decreased the resistance of cartilage to being deformed under fast dynamic and quasi-static loading. The dynamic moduli of GAG-depleted cartilage were smaller than those of intact cartilage (Fig. 3b). This suggests that GAG-depleted cartilage undergoes large deformation under the same pressure generated by high-frequency loading. The decreased resistance under high-frequency loading after GAG depletion (Fig. 3b) could be attributed to relatively decreased lateral expansion of cartilage (i.e., less volumetric change)

due to the increased diffusivity, resulting in a decrease in the tensile strain of collagen fibrils (Andriotis et al., 2018; Han et al., 2019, 2018; Wong et al., 2000). In addition, the sharp decrease in equilibrium modulus as a function of the solid matrix integrity (Fig. 2c) showed that GAG-depleted cartilage could not resist quasi-static compression as much as intact cartilage. This was likely because the loss of negatively charged GAGs decreased osmotic pressure and repulsive force between charge groups, as shown in previous studies (Eisenberg and Grodzinsky, 1985; Mow et al., 1992; Qin et al., 2002; Wahlquist et al., 2017). The effects of GAG depletion on moduli were much larger under quasi-static loading than high-frequency loading. These findings suggest that cartilage could gradually lose the ability to resist dynamic and quasi-static loading at the early stages of osteoarthritis, where GAG loss occurs.

The current study, combined with previous studies, provides a map of cartilage dissipative responses across multiple length- and time-scales (Fig. 4). This study filled the gap in high-frequency macroscopic dissipative responses of cartilage as a function of the solid matrix integrity, offering fundamental insight into cartilage dissipative behavior under traumatic scenarios at a contact length experienced in vivo (Chan et al., 2016; Fukubayashi and Kurosawa, 1980). Cartilage dissipation comes from the combination of PE and VE dissipation mechanisms (Akizuki et al., 1986; Boettcher et al., 2016; Han et al., 2018; Matthews et al., 1977; Nia et al., 2011). While PE dissipation depends on the square of the characteristic diffusion length and loading frequency (Lai and Hu, 2017; Nia et al., 2011), VE dissipation only depends on the loading frequency. Hence, the frequency axis was normalized by the square of the length to eliminate the dependency of PE dissipation on the length (Han et al., 2018; Lai and Hu, 2017) so that cartilage dissipative responses measured at different length- and time-scales were compared on a common scale. The frequencies of three dissipation peak values from intact cartilage (Han et al., 2018; Nia et al., 2011, 2013) collapsed into a nearly single value after the normalization (Fig. 4). The ratio of the highest to the lowest frequencies of the peak values was around 11 before the normalization, whereas the ratio dropped to around 2 after the normalization. As a result, the dissipation peak values were aligned near  $a^2 f \approx 1 \times 10^{-9}$  m<sup>2</sup>/s. The collapse of the frequencies after the normalization indicated that PE dissipation dominantly governs intact cartilage dissipation around the peak values (Lai and Hu, 2017), consistent with the findings of the corresponding previous studies (Han et al., 2018; Nia et al., 2011, 2013). Beyond the dominant PE peaks, the contribution of PE dissipation to total dissipation decreases toward the right side of the normalized axis as the length and frequency increase. In particular, previous work with multiscale dynamic testing showed that VE dissipation becomes a dominant dissipation mechanism of intact cartilage after a normalized frequency of around  $4 \times 10^{-9}$  m<sup>2</sup>/s (Han

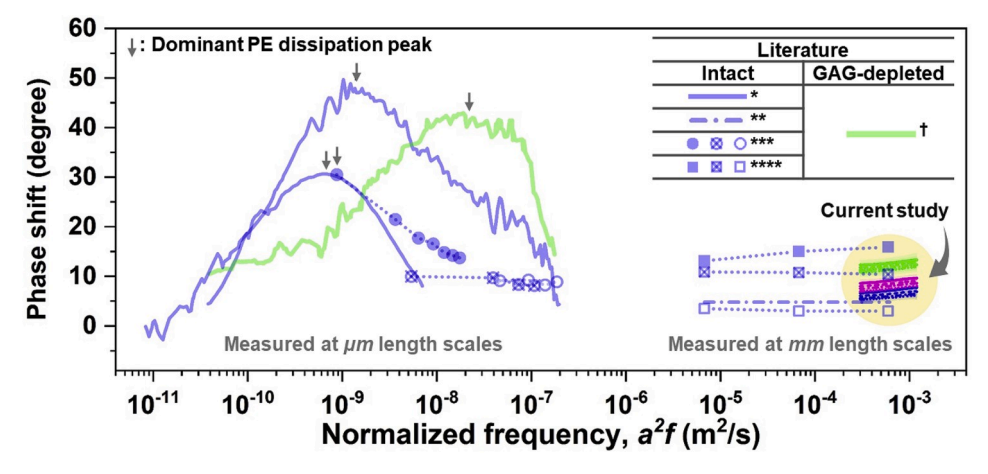


Fig. 4. Dissipative responses of intact and GAG-depleted cartilage at multiple length- and time-scales. These responses were obtained under small-amplitude normal oscillations. The standard deviations for previous data (\*(Nia et al., 2011, 2013), \*\*(Fulcher et al., 2009), \*\*\*(Han et al., 2018), \*\*\*\*(Lawless et al., 2017), and †(Nia et al., 2013)) are not presented. Arrows indicate dominant PE dissipation peaks. The legend for the current findings is presented in Fig. 3.

et al., 2018). In addition, an analytical solution for oscillatory indenters on PE materials showed that PE dissipation sharply decreases within two decades from the normalized frequency of a peak value (Lai and Hu, 2017). Consequently, the current study combined with the previous studies and high Peclet numbers showed that macroscopic high-frequency dissipative behavior of intact cartilage dominantly derived from VE dissipation. GAG depletion shifts the normalized frequency of the PE dissipation peak to around  $2 \times 10^{-8}$  m<sup>2</sup>/s (Nia et al., 2013) due to the increased diffusivity. The current results of GAG-depleted cartilage were placed much more than two decades from the previously reported PE peak. Therefore, this suggests that VE dissipation is likely to govern macroscopic high-frequency dissipation of GAG-depleted cartilage, which is consistent with the estimated Peclet numbers for both intact and GAG-depleted cartilage. The findings regarding GAG-depleted cartilage provided the effect of the solid matrix integrity on high-frequency microscopic dissipation, which was not previously explored. Some discrepancies between results from different studies could be due to the differences in the age and species of samples and the experimental testing conditions. The dissipation map can be used to predict cartilage dissipation capacity across wide ranges of loading frequencies and length scales.

This study has a few limitations. The test conditions do not exactly represent in vivo conditions; however, DMA and stress relaxation tests provided dissipative and mechanical properties of cartilage at a macroscopic length scale, comparable to contact lengths in the native joints in vivo (Chan et al., 2016; Fukubayashi and Kurosawa, 1980), as a function of the solid matrix integrity. The dissipative responses of cartilage in this study, as well as in previous studies, were measured under small-amplitude oscillatory compression. Therefore, they cannot represent cartilage dissipation under large-amplitude oscillatory compression accompanying nonlinear behavior. While the predominant dissipation mechanism evaluated in this study is argued to be intrinsic VE dissipation, potential irreversible causes of energy loss that could contribute to the low phase angles include tissue reorganization and irreversible breaking of molecular bonds (Jung et al., 2015; Linka et al., 2018). If present, these mechanisms would imply that damage occurs under physiological deformation in articular cartilage. The dissipation map across multiple length- and time-scales is composed of intact and GAG-depleted cartilage from large species (bovine and porcine cartilage), and therefore it describes dissipative behavior of macroscale cartilage; the easy controllability of the sample size enables dynamic testing from micro-to macro-scales. Previous studies showed that GAG depletion of cartilage from small species (murine cartilage with microscale thickness) induces relatively low poroelastic peak values and small shifts of the peak frequencies in comparison to cartilage from large species (Azadi et al., 2016; Han et al., 2019; Nia et al., 2015); dissipation behavior of intact cartilage from small species was similar to that from large species. It was shown that the differences in GAG-depleted cartilage dissipation responses were because the ability of GAG-depleted cartilage from small species to maintain the fluid pressurization and self-stiffening behavior is less strong than that from large species (Nia et al., 2015). Osteoarthritis-like cartilage damage was simulated by degrading the non-fibrillar matrix via the treatment of trypsin. Thus, the current results do not explain osteoarthritis accompanied by the degeneration of the collagen fibrillar matrix.

# 5. Conclusions

This study investigated dissipative and mechanical responses of intact and osteoarthritis-like cartilage at a macroscopic length in a previously unexplored high-frequency range. Different degrees of GAG depletion were induced via trypsin enzymatic digestion of cartilage. Under high-frequency loading consistent with traumatic impact, the energy dissipation of cartilage increased with the degeneration of the solid matrix and decreased with strain. An increase in cartilage dissipation capacity after GAG depletion was likely caused by increased

viscoelastic dissipation. In addition, the resistance of cartilage to being deformed decreased with the degree of GAG depletion. Under quasistatic loading consistent with human beings at rest, GAG-depleted cartilage relaxed much faster and lost compressive strength in equilibrium in comparison to intact cartilage. Sharply decreased relaxation times after the GAG depletion were thought to be mainly due to an increased diffusivity. These dissipative and mechanical properties measured at a contact length comparable to the native joints *in vivo* filled the knowledge gaps about dissipative and mechanical properties of intact and GAG depleted cartilage in an unprecedented high-frequency range. In particular, they lay the foundation for interpreting energy dissipation associated with cartilage failure as a function of the solid matrix integrity under traumatic injury and high-rate physiological loading.

#### CRediT authorship contribution statement

Guebum Han: Conceptualization, Data curation, Formal analysis, Investigation, Methodology, Project administration, Visualization, Writing - original draft, Writing - review & editing. Utku Boz: Conceptualization, Methodology, Supervision, Writing - review & editing. Melih Eriten: Conceptualization, Funding acquisition, Methodology, Project administration, Resources, Supervision, Writing - original draft, Writing - review & editing. Corinne R. Henak: Conceptualization, Funding acquisition, Methodology, Project administration, Resources, Supervision, Validation, Writing - original draft, Writing - review & editing.

#### Acknowledgment

Funding from the National Science Foundation (CMMI-DCSD-1662456) is gratefully acknowledged. We are grateful to Shannon K. Walsh for helpful discussions on statistical analysis.

# References

- Akizuki, S., Mow, V.C., Müller, F., Pita, J.C., Howell, D.S., Manicourt, D.H., 1986. Tensile properties of human knee joint cartilage: I. Influence of ionic conditions, weight bearing, and fibrillation on the tensile modulus. J. Orthop. Res. 4, 379–392. https://doi.org/10.1002/jor.1100040401.
- Andriotis, O.G., Desissaire, S., Thurner, P.J., 2018. Collagen fibrils: nature's highly tunable nonlinear springs. ACS Nano 12, 3671–3680. https://doi.org/10.1021/acsnano.8b00837
- Azadi, M., Nia, H.T., Gauci, S.J., Ortiz, C., Fosang, A.J., Grodzinsky, A.J., 2016. Wide bandwidth nanomechanical assessment of murine cartilage reveals protection of aggrecan knock-in mice from joint-overuse. J. Biomech. 49, 1634–1640. https://doi. org/10.1016/j.jbiomech.2016.03.055.
- Bartell, L.R., Xu, M.C., Bonassar, L.J., Cohen, I., 2018. Local and global measurements show that damage initiation in articular cartilage is inhibited by the surface layer and has significant rate dependence. J. Biomech. https://doi.org/10.1016/j. ibiomech.2018.02.033.
- Boettcher, K., Kienle, S., Nachtsheim, J., Burgkart, R., Hugel, T., Lieleg, O., 2016. The structure and mechanical properties of articular cartilage are highly resilient towards transient dehydration. Acta Biomater. 29, 180–187. https://doi.org/10.1016/j.actbio.2015.09.034.
- Bonassar, L.J., Frank, E.H., Murray, J.C., Paguio, C.G., Moore, V.L., Lark, M.W., Sandy, J. D., Wu, J.-J., Eyre, D.R., Grodzinsky, A.J., 1995. Changes in cartilage composition and physical properties due to stromelysin degradation. Arthritis Rheum. 38, 173–183. https://doi.org/10.1002/grt.1780380205.
- Chan, D.D., Cai, L., Butz, K.D., Trippel, S.B., Nauman, E.A., Neu, C.P., 2016. In vivo articular cartilage deformation: noninvasive quantification of intratissue strain during joint contact in the human knee. Sci. Rep. 6, 19220. https://doi.org/ 10.1038/srep19220.
- DiDomenico, C.D., Lintz, M., Bonassar, L.J., 2018. Molecular transport in articular cartilage — what have we learned from the past 50 years? Nat. Rev. Rheumatol. 14, 393. https://doi.org/10.1038/s41584-018-0033-5.
- Edelsten, L., Jeffrey, J.E., Burgin, L.V., Aspden, R.M., 2010. Viscoelastic deformation of articular cartilage during impact loading. Soft Matter 6, 5206–5212. https://doi.org/ 10.1039/C0SM00097C.
- Eisenberg, S.R., Grodzinsky, A.J., 1985. Swelling of articular cartilage and other connective tissues: electromechanochemical forces. J. Orthop. Res. 3, 148–159. https://doi.org/10.1002/jor.1100030204.
- Fukubayashi, T., Kurosawa, H., 1980. The contact area and pressure distribution pattern of the knee: a study of normal and osteoarthrotic knee joints. Acta Orthop. Scand. 51, 871-879. https://doi.org/10.3109/17453678008990887.

- Fulcher, G.R., Hukins, D.W.L., Shepherd, D.E.T., 2009. Viscoelastic properties of bovine articular cartilage attached to subchondral bone at high frequencies. BMC Muscoskel. Disord. 10, 61. https://doi.org/10.1186/1471-2474-10-61.
- Griffin, D.J., Vicari, J., Buckley, M.R., Silverberg, J.L., Cohen, I., Bonassar, L.J., 2014. Effects of enzymatic treatments on the depth-dependent viscoelastic shear properties of articular cartilage. J. Orthop. Res. 32, 1652–1657. https://doi.org/10.1002/ jor.20713
- Han, B., Li, Q., Wang, C., Patel, P., Adams, S.M., Doyran, B., Nia, H.T., Oftadeh, R., Zhou, S., Li, C.Y., Liu, X.S., Lu, X.L., Enomoto-Iwamoto, M., Qin, L., Mauck, R.L., Iozzo, R.V., Birk, D.E., Han, L., 2019. Decorin regulates the aggrecan network integrity and biomechanical functions of cartilage extracellular matrix. ACS Nano 13, 11320–11333. https://doi.org/10.1021/acsnano.9b04477.
- Han, E., Chen, S.S., Klisch, S.M., Sah, R.L., 2011. Contribution of proteoglycan osmotic swelling pressure to the compressive properties of articular cartilage. Biophys. J. 101, 916–924. https://doi.org/10.1016/j.bpj.2011.07.006.
- Han, G., Eriten, M., Henak, C.R., 2019. Rate-dependent crack nucleation in cartilage under microindentation. J. Mech. Behav. Biomed. Mater. 96, 186–192. https://doi. org/10.1016/j.jmbbm.2019.04.015.
- Han, G., Hess, C., Eriten, M., Henak, C.R., 2018. Uncoupled poroelastic and intrinsic viscoelastic dissipation in cartilage. J. Mech. Behav. Biomed. Mater. 84, 28–34. https://doi.org/10.1016/j.jmbbm.2018.04.024.
- Han, L., Frank, E.H., Greene, J.J., Lee, H.-Y., Hung, H.-H.K., Grodzinsky, A.J., Ortiz, C., 2011. Time-dependent nanomechanics of cartilage. Biophys. J. 100, 1846–1854. https://doi.org/10.1016/j.bpj.2011.02.031.
- Henak, C.R., Bartell, L.R., Cohen, I., Bonassar, L.J., 2017. Multiscale strain as a predictor of impact-induced fissuring in articular cartilage. J. Biomech. Eng. 139, 031004 https://doi.org/10.1115/1.4034994.
- Hu, Y., Zhao, X., Vlassak, J.J., Suo, Z., 2010. Using indentation to characterize the poroelasticity of gels. Appl. Phys. Lett. 96, 121904. https://doi.org/10.1063/ 1.3370354.
- Huang, C.-Y., Soltz, M.A., Kopacz, M., Mow, V.C., Ateshian, G.A., 2003. Experimental verification of the roles of intrinsic matrix viscoelasticity and tension-compression nonlinearity in the biphasic response of cartilage. J. Biomech. Eng. 125, 84–93. https://doi.org/10.1115/1.1531656.
- Huang, Y.-P., Zheng, Y.-P., 2009. Intravascular ultrasound (IVUS): a potential arthroscopic tool for quantitative assessment of articular cartilage. Open Biomed. Eng. J. 3, 13–20. https://doi.org/10.2174/1874120700903010013.
- June, R.K., Ly, S., Fyhrie, D.P., 2009. Cartilage stress-relaxation proceeds slower at higher compressive strains. Arch. Biochem. Biophys. 483, 75–80. https://doi.org/ 10.1016/j.abb.2008.11.029.
- Jung, G., Qin, Z., Buehler, M.J., 2015. Mechanical properties and failure of biopolymers: atomistic reactions to macroscale response. Top. Curr. Chem. 369, 317–343. https://doi.org/10.1007/128.2015.643.
- Kaplan, J.T., Neu, C.P., Drissi, H., Emery, N.C., Pierce, D.M., 2017. Cyclic loading of human articular cartilage: the transition from compaction to fatigue. J. Mech. Behav. Biomed. Mater. 65, 734–742. https://doi.org/10.1016/j.jmbbm.2016.09.040.
- Kempson, G.E., Freeman, M.a.R., Swanson, S.a.V., 1968. Tensile properties of articular cartilage. Nature 220, 1127–1128. https://doi.org/10.1038/2201127b0.
- Kiviranta, P., Rieppo, J., Korhonen, R.K., Julkunen, P., Töyräs, J., Jurvelin, J.S., 2006. Collagen network primarily controls Poisson's ratio of bovine articular cartilage in compression. J. Orthop. Res. 24, 690–699. https://doi.org/10.1002/jor.20107.
- Korhonen, R.K., Laasanen, M.S., Töyräs, J., Rieppo, J., Hirvonen, J., Helminen, H.J., Jurvelin, J.S., 2002. Comparison of the equilibrium response of articular cartilage in unconfined compression, confined compression and indentation. J. Biomech. 35, 903–909. https://doi.org/10.1016/S0021-9290(02)00052-0.
- Lai, Y., Hu, Y., 2017. Unified solution for poroelastic oscillation indentation on gels for spherical, conical and cylindrical indenters. Soft Matter 13, 852–861. https://doi. org/10.1039/C6SM02341J.
- Lakes, P.R., 2009. Viscoelastic Materials, 1 edition. Cambridge University Press, Cambridge; New York.
- Lawless, B.M., Sadeghi, H., Temple, D.K., Dhaliwal, H., Espino, D.M., Hukins, D.W.L., 2017. Viscoelasticity of articular cartilage: analysing the effect of induced stress and the restraint of bone in a dynamic environment. J. Mech. Behav. Biomed. Mater. 75, 293–301. https://doi.org/10.1016/j.jmbbm.2017.07.040.
- Lewis, JackL., Johnson, S.L., 2001. Collagen architecture and failure processes in bovine patellar cartilage. J. Anat. 199, 483–492. https://doi.org/10.1046/j.1469-7580.2001.19940483.x.

- Linka, K., Hillgärtner, M., Itskov, M., 2018. Fatigue of soft fibrous tissues: multi-scale mechanics and constitutive modeling. Acta Biomater. 71, 398–410. https://doi.org/ 10.1016/j.actbio.2018.03.010.
- Mak, A.F., 1986. The apparent viscoelastic behavior of articular cartilage—the contributions from the intrinsic matrix viscoelasticity and interstitial fluid flows. J. Biomech. Eng. 108, 123–130. https://doi.org/10.1115/1.3138591.
- Maroudas, A., Wachtel, E., Grushko, G., Katz, E.P., Weinberg, P., 1991. The effect of osmotic and mechanical pressures on water partitioning in articular cartilage. Biochim. Biophys. Acta BBA - Gen. Subj. 1073, 285–294. https://doi.org/10.1016/ 0304.4165(91)90133-2
- Matthews, L.S., Sonstegard, D.A., Henke, J.A., 1977. Load bearing characteristics of the patello-femoral joint. Acta Orthop. Scand. 48, 511–516. https://doi.org/10.3109/ 17453677708989740
- Mow, V.C., Kuei, S.C., Lai, W.M., Armstrong, C.G., 1980. Biphasic creep and stress relaxation of articular cartilage in compression: theory and experiments. J. Biomech. Eng. 102, 73–84. https://doi.org/10.1115/1.3138202.
- Mow, V.C., Ratcliffe, A., Robin Poole, A., 1992. Cartilage and diarthrodial joints as paradigms for hierarchical materials and structures. Biomaterials 13, 67–97. https:// doi.org/10.1016/0142-9612(92)90001-5.
- Nguyen, Q., Murphy, G., Roughley, P.J., Mort, J.S., 1989. Degradation of proteoglycan aggregate by a cartilage metalloproteinase. Evidence for the involvement of stromelysin in the generation of link protein heterogeneity in situ. Biochem. J. 259, 61–67.
- Nia, H., Bozchalooi, I.S., Li, Y., Han, L., Hung, H.-H., Frank, E., Youcef-Toumi, K., Ortiz, C., Grodzinsky, A., 2013. High-bandwidth AFM-based rheology reveals that cartilage is most sensitive to high loading rates at early stages of impairment. Biophys. J. 104, 1529–1537. https://doi.org/10.1016/j.bpj.2013.02.048.
- Nia, H., Han, L., Li, Y., Ortiz, C., Grodzinsky, A., 2011. Poroelasticity of cartilage at the nanoscale. Biophys. J. 101, 2304–2313. https://doi.org/10.1016/j.bpj.2011.09.011.
- Nia, H., Han, L., Soltani Bozchalooi, I., Roughley, P., Youcef-Toumi, K., Grodzinsky, A.J., Ortiz, C., 2015. Aggrecan nanoscale solid–fluid interactions are a primary determinant of cartilage dynamic mechanical properties. ACS Nano 9, 2614–2625. https://doi.org/10.1021/nn5062707.
- Nia, H.T., Gauci, S.J., Azadi, M., Hung, H.-H., Frank, E., Fosang, A.J., Ortiz, C., Grodzinsky, A.J., 2015. High-bandwidth AFM-based rheology is a sensitive indicator of early cartilage aggrecan degradation relevant to mouse models of osteoarthritis. J. Biomech. 48, 162–165. https://doi.org/10.1016/j.jbiomech.2014.11.012.
- Park, S., Nicoll, S.B., Mauck, R.L., Ateshian, G.A., 2008. Cartilage mechanical response under dynamic compression at physiological stress levels following collagenase digestion. Ann. Biomed. Eng. 36, 425–434. https://doi.org/10.1007/s10439-007-04316
- Qin, L., Zheng, Y., Leung, C., Mak, A., Choy, W., Chan, K., 2002. Ultrasound detection of trypsin-treated articular cartilage: its association with cartilaginous proteoglycans assessed by histological and biochemical methods. J. Bone Miner. Metabol. 20, 281–287. https://doi.org/10.1007/s007740200040.
- Quinn, T.M., Allen, R.G., Schalet, B.J., Perumbuli, P., Hunziker, E.B., 2001. Matrix and cell injury due to sub-impact loading of adult bovine articular cartilage explants: effects of strain rate and peak stress. J. Orthop. Res. 19, 242–249. https://doi.org/ 10.1016/S0736-0266(00)00025-5.
- Sadeghi, H., Shepherd, D.E.T., Espino, D.M., 2015. Effect of the variation of loading frequency on surface failure of bovine articular cartilage. Osteoarthritis Cartilage 23, 2252–2258. https://doi.org/10.1016/j.joca.2015.06.002.
- Schmidt, M.B., Mow, V.C., Chun, L.E., Eyre, D.R., 1990. Effects of proteoglycan extraction on the tensile behavior of articular cartilage. J. Orthop. Res. 8, 353–363. https://doi.org/10.1002/jor.1100080307.
- Soulhat, J., Buschmann, M.D., Shirazi-Adl, A., 1999. A fibril-network-reinforced biphasic model of cartilage in unconfined compression. J. Biomech. Eng. 121, 340–347. https://doi.org/10.1115/1.2798330.
- Torzilli, P.A., 1985. Influence of cartilage conformation on its equilibrium water partition. J. Orthop. Res. 3, 473–483. https://doi.org/10.1002/jor.1100030410.
- Wahlquist, J.A., DelRio, F.W., Randolph, M.A., Aziz, A.H., Heveran, C.M., Bryant, S.J., Neu, C.P., Ferguson, V.L., 2017. Indentation mapping revealed poroelastic, but not viscoelastic, properties spanning native zonal articular cartilage. Acta Biomater. 64, 41–49. https://doi.org/10.1016/j.actbio.2017.10.003.
- Wong, M., Ponticiello, M., Kovanen, V., Jurvelin, J.S., 2000. Volumetric changes of articular cartilage during stress relaxation in unconfined compression. J. Biomech. 33, 1049–1054. https://doi.org/10.1016/S0021-9290(00)00084-1.